Electronic Supplementary Information

Experimental section

Materials:

Titanium mesh (TM) was obtained from Qingyuan Metal Material Ltd. (Taixing, China). Potassium nitrate (KNO_3 ≥ 99.0%), potassium nitrate isotope ($K^{15}NO_3$ ≥ 98.5%), potassium nitrite (KNO_2 ≥ 9.0%), potassium sulfate (K_2SO_4 ≥ 99.0%), ammonium chloride (NH_4Cl ≥ 99.5%) potassium hydroxide (KOH ≥ 99.0%), sodium salicylate ($C_7H_5NaO_3$, 99.0%), trisodium citrate dihydrate ($C_6H_5Na_3O_7·2H_2O$, 99.0%), p-dimethylaminobenzaldehyde ($C_9H_{11}NO$, AR), sodium nitroferricyanide dihydrate ($C_5FeN_6Na_2O·2H_2O$, 99.0%), sulfamic acid solution (H_3NO_3S, 0.8 wt%) and sodium hypochlorite solution (NaClO, 4.0 wt%) Nitrobenzene Standard ($C_6H_5NO_2$, AR) weer purchased from Aladdin Ltd. (Shanghai, China). Sodium hexachloroiridate(III) hydrate ($Na_3IrCl_6·xH_2O$, Ir 35%~40%) and Cobalt chloride hexahydrate ($CoCl_2·6H_2O$, AR) were purchased from Chengdu Kelong Chemical Reagent Co. Ltd. Sulfuric acid (H_2SO_4, 95.0%~98.0%), hydrogen peroxide (H_2O_2, ≥ 30%), hydrochloric acid (HCl, 36.0%~38.0%), hydrazine monohydrate ($N_2H_4·H_2O$，> 98.0%) and ethyl alcohol (C_2H_5OH, 99.5%) were bought from Beijing Chemical Corporation. (China). chemical Ltd. in Chengdu. Aniline (C_6H_7N, 99+%) were bought from Alfa Aesar (China) chemical Ltd. All reagents used in this work were analytical grade without further purification.

Characterizations:

XRD data were acquired by a LabX XRD-6100 X-ray diffractometer with a Cu Kα radiation (40 kV, 30 mA) of wavelength 0.154 nm (SHIMADZU, Japan). SEM measurements were carried out on a GeminiSEM 300 scanning electron microscope (ZEISS, Germany) at an accelerating voltage of 5 kV. XPS measurements were performed on an ESCALABMK II X-ray photoelectron spectrometer using Mg as the exciting source. The absorbance data of the spectrophotometer was measured on a UV-Vis spectrophotometer. TEM image was obtained from a Zeiss Libra 200FE transmission electron microscope operated at 200 kV. 1H NMR spectra were

collected on Varian VNMRS 600 MHz (the USA). GC results were obtained from GC-2010 pro.

Determination of NH_3:

The concentration of produced NH_3 was determined by spectrophotometry measurement with the indophenol blue method (the obtained electrolyte was diluted 50 times) [1]. In detail, 2 mL of the diluted catholyte was obtained from the cathodic chamber and mixed with 2 mL of a 1 M NaOH solution that contained salicylic acid and sodium citrate. Then, 1 mL of 0.05 M NaClO and 0.2 mL of 1 wt% $C_5FeN_6Na_2O$ were dropped into the collected electrolyte solution. After standing at room temperature for 2 h, the ultraviolet-visible absorption spectrum was measured. The concentration-absorbance curve was calibrated using the standard NH_4Cl solution with NH_3 concentrations of 0.5, 1.0, 2.0, 3.0, 4.0 and 5.0 ppm in 0.1 M KOH. The absorbance at 655 nm was measured to quantify the NH_3 concentration using standard NH_4Cl solutions ($y = 0.37315\ x + 0.05594$, $R^2 = 0.999$).

Determination of NO_2^-:

The NO_2^- concentration was analyzed using the Griess test [2]. The Griess reagent was prepared by dissolving 0.1 g N-(1-naphthyl) ethylenediamine dihydrochloride, 1.0 g sulfonamide and 2.94 mL H_3PO_4 in 50 mL deionized water. In a typical colourimetric assay, the 1.0 mL Griess reagent was mixed with the 1.0 mL nitrite-containing solution and 2.0 mL H_2O and allowed to react at room temperature for 10 min, in which sulfonamide reacts with NO_2^- to form a diazonium salt and then further reacts with the amine to form an azo dye (magenta). The absorbance at 540 nm was measured to quantify the NO_2^- concentration with a standard curve of NO_2^- ($y = 0.20024\ x + 0.00407$, $R^2 = 0.999$).

Determination of N_2H_4:

In this work, we used the method of Watt and Chrisp [3] to determine the concentration of produced N_2H_4. The chromogenic reagent was a mixed solution of

5.99 g $C_9H_{11}NO$, 30 mL HCl and 300 mL C_2H_5OH. In detail, 1 mL electrolyte was added into 1 mL prepared colour reagent and stirred for 15 min in the dark. The absorbance at 455 nm was measured to quantify the N_2H_4 concentration with a standard curve of hydrazine ($y = 1.07368\ x + 0.02127$, $R^2 = 0.999$).

^{15}N isotope labeling experiments:

$K^{15}NO_3$ was used as the feeding N-source for the isotopic labeling nitrate reduction experiments to clarify the source of ammonia. After electrolysis in 0.1 M KOH with 0.1 M $^{15}NO_3^-$ or $^{14}NO_3^-$ at -0.2 V for 1 h, the H value of the obtained electrolyte was adjusted to 2.0 by adding 0.1 M HCl solution. Then, 0.5 mL of electrolyte and 0.05 mL of D_2O were added into the ^{1}HNMR tube for further ^{1}HNMR

Calculations of FE and NH_3 yield:

$$FE = (8 \times F \times [NH_3] \times V) / (M_{NH_3} \times Q) \times 100\%$$

$$NH_3\ yield = ([NH_3] \times V) / ((M_{NH_3} \times t \times A)$$

Where F is the Faradic constant (96485 C mol^{-1}), $[NH_3]$ is the measured NH_3 concentration, V is the volume of electrolyte in the anode compartment (50 mL), M_{NH_3} is the molar mass of NH_3, Q is the total quantity of applied electricity, t is the electrolysis time and A is the loaded area of catalyst (0.5 × 0.5 cm^2).

Calculations of FE and NO_2^- yield:

$$FE = (2 \times F \times [NO_2^-] \times V) / (M_{NO2-} \times Q) \times 100\%$$

$$NO_2^-\ yield = ([NO_2^-] \times V) / ((M_{NO2-} \times t \times A)$$

Where F is the Faradic constant (96485 C mol^{-1}), $[NO_2^-]$ is the measured NO_2^- concentration, V is the volume of electrolyte in the anode compartment (50 mL), M_{NO2-} is the molar mass of NO_2^-, Q is the total quantity of applied electricity, t is the electrolysis time and A is the loaded area of catalyst (0.5 × 0.5 cm^2).

Ph-NO_2 ERR： The electrolyte was collected and extracted with ethylacetate after i-t tests. The extracted products were determined by comparing the GC retention times and mass spectra. The Ph-NO_2 conversion and Ph-NH_2 yield were acquired via the GC results analysis and calculated based on the following

Conversion = mol of the consumed Ph-NO_2 / mole of the added Ph-NO_2 × 100%

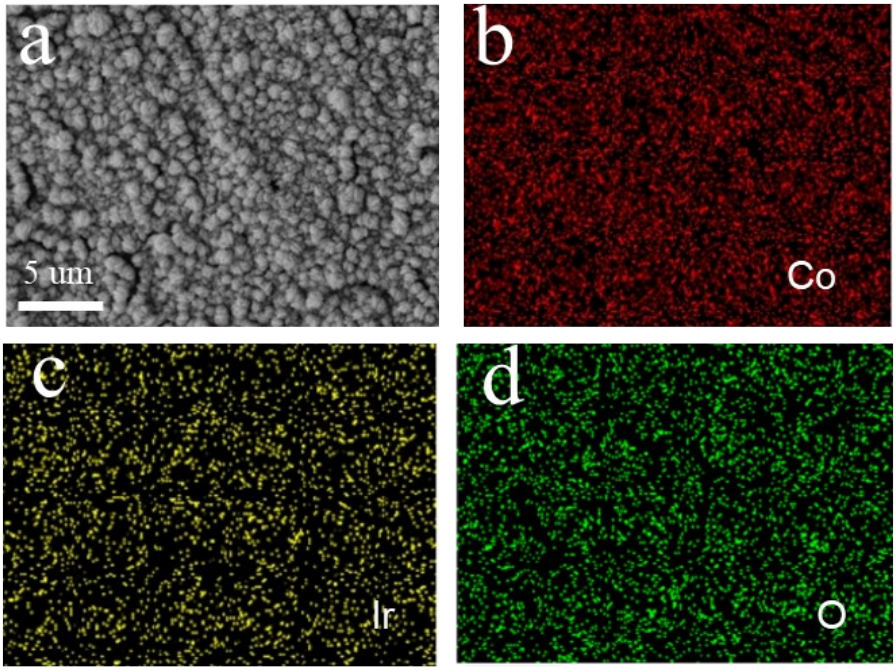

Fig. S1. (a) SEM image of Ir@$Co(OH)_2$/TM. EDX mapping image of (b) Co, (c)I r and (d) O of Ir@$Co(OH)_2$/TM.

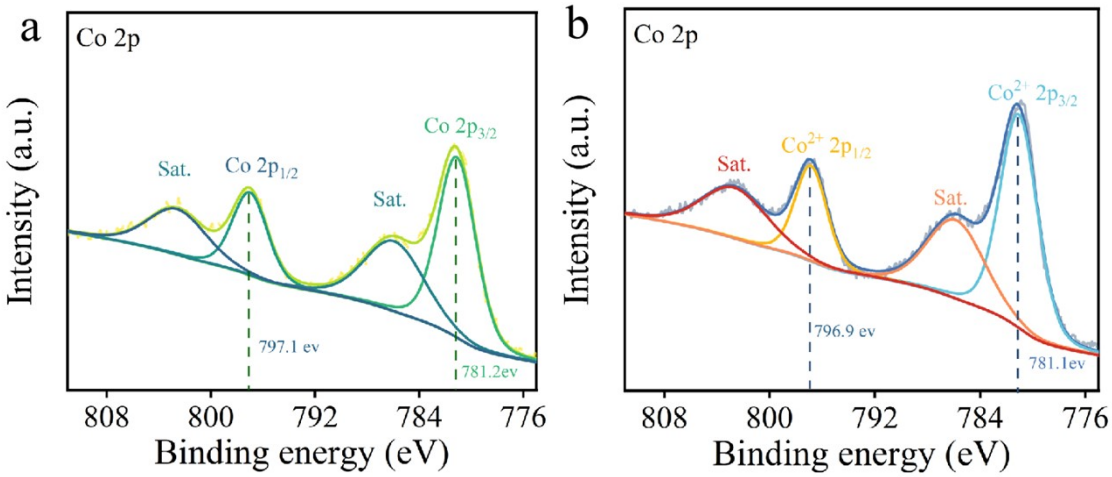

Fig. S2. XPS spectra of (a) $Co(OH)_2$/TM in the Co 2p region and (b) Ir@$Co(OH)_2$/TM in the Co 2p region.

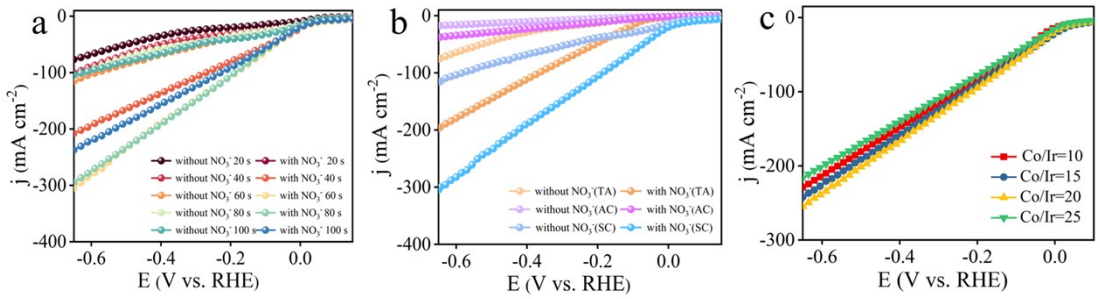

Fig. S3. LSV curves of Ir@$Co(OH)_2$/TM samples prepared at different (a) electrodeposition time; (b) different ligands in 0.1 M KOH with 0.1 M KNO_3; (c) different Co/Ir molar ratio.

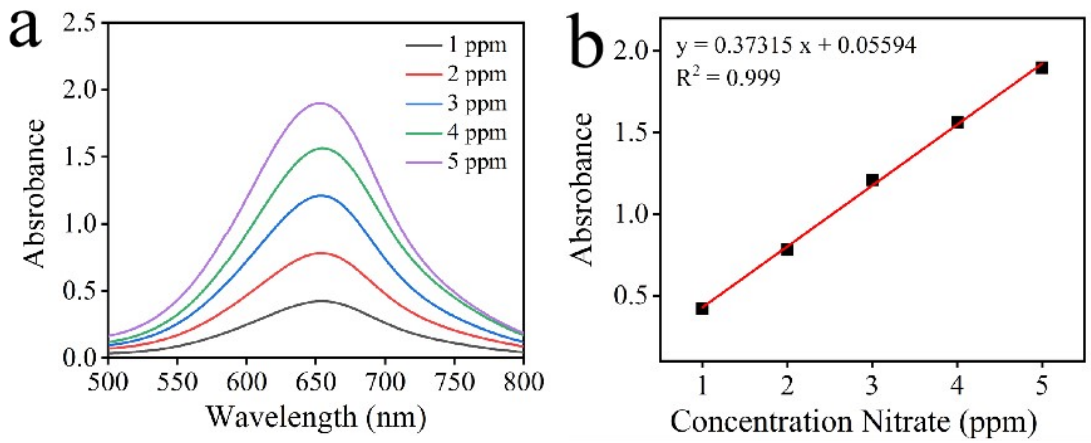

Fig. S4. (a) UV-Vis absorption spectra of indophenol assays kept with different concentrations of NH_4^+ after incubated for 2 h at room temperature; (b) Calibration curve used for estimation of NH_4^+ concentration.

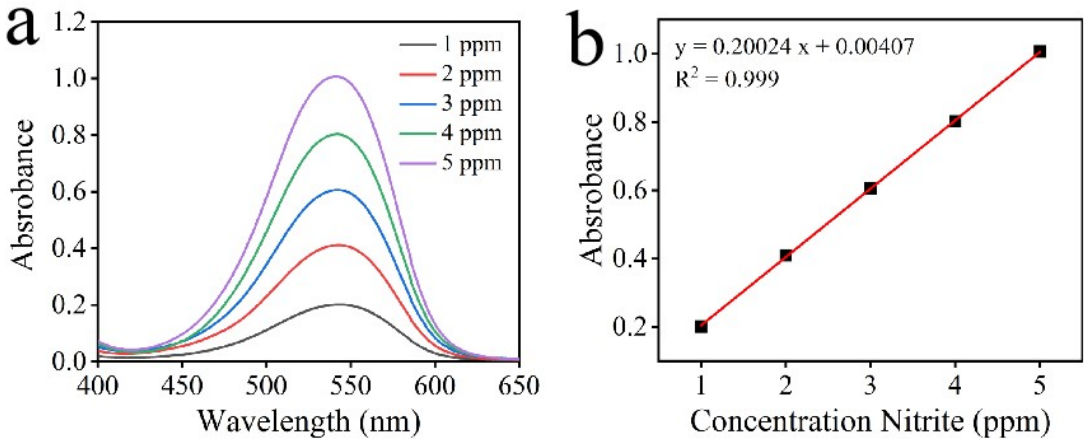

Fig. S5. UV-Vis absorption spectra of various NO_2^- concentrations after incubated for 10 min at room temperature; (b) Calibration curve used for quantification of NO_2^- concentration.

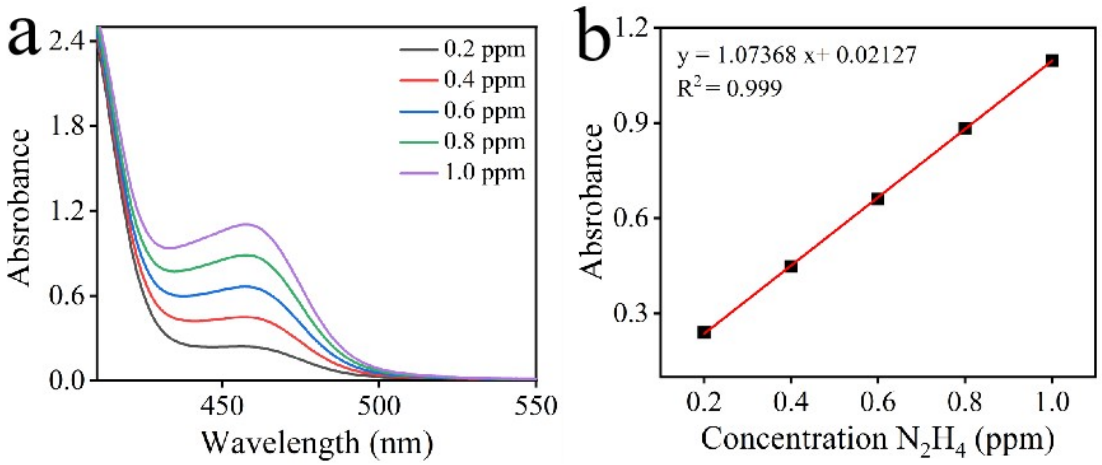

Fig. S6. (a) UV-Vis absorption spectra of various N_2H_4 concentrations after incubated for 15 min at room temperature; (b) Calibration curve used for calculation of N_2H_4 concentration.

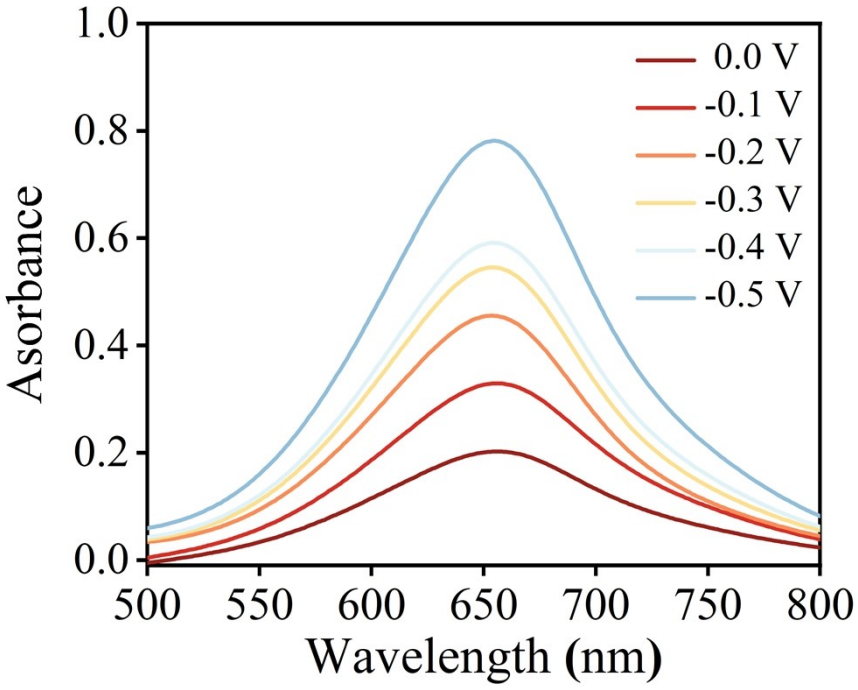

Fig. S7. (a) UV-Vis spectra of NH_3 generated on Ir@$Co(OH)_2$/TM at different given potentials in the 0.1 M KOH with 0.1 M NO_3^-.

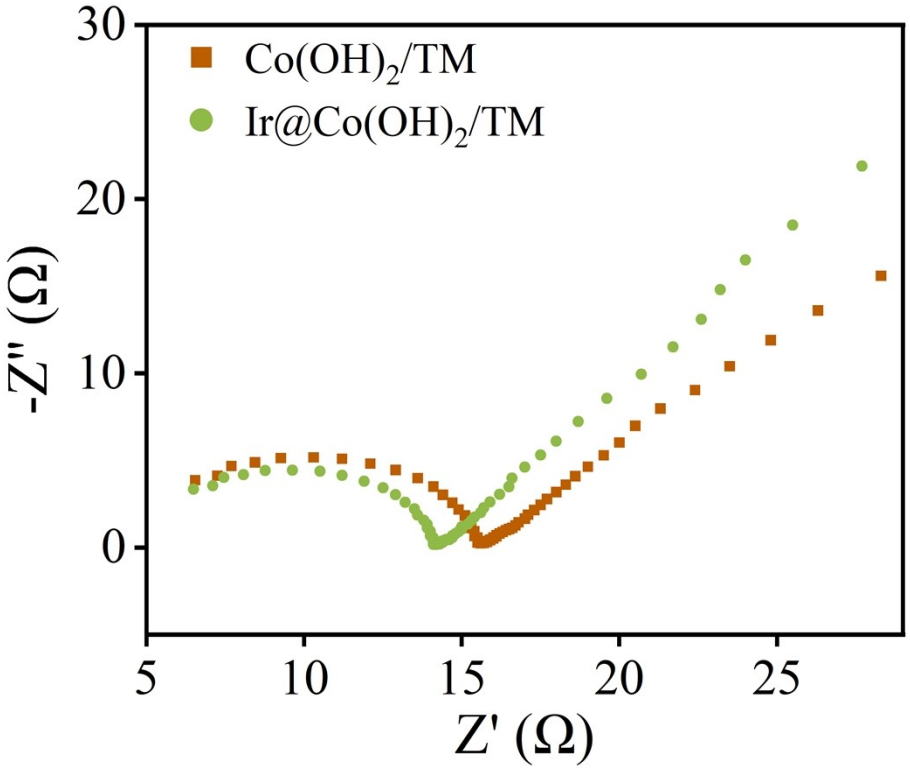

Fig. S8. Nyquist plots of different samples

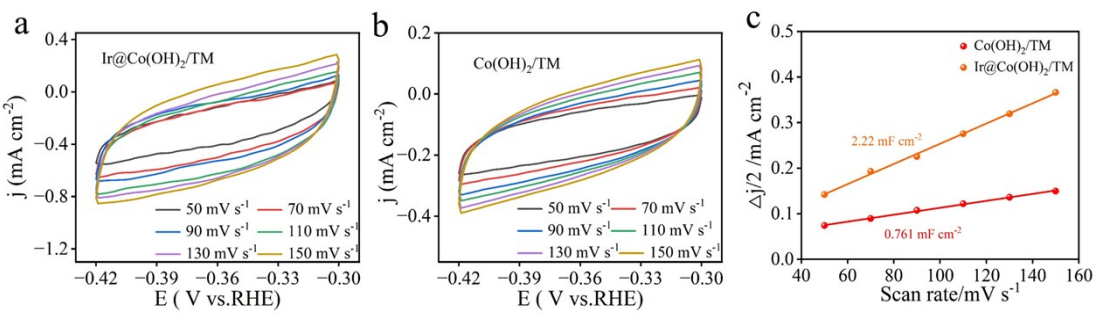

Fig. S9. The CV profiles obtained with (a) Ir@$Co(OH)_2$/TM and (b) $Co(OH)_2$/TM at different scan rates from 50 mV/s to 150 mV/s. (c) The corresponding fitting results of C_{dl}.

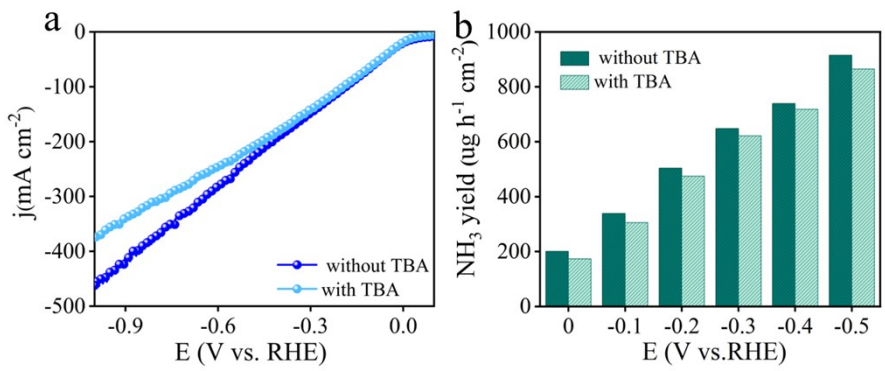

Fig. S10. (a) Different LSV curves of Ir@$Co(OH)_2$/TM with or without TBA; (b) NH_3 yields and FEs of Ir@$Co(OH)_2$/TM from 0 V to -0.5 V

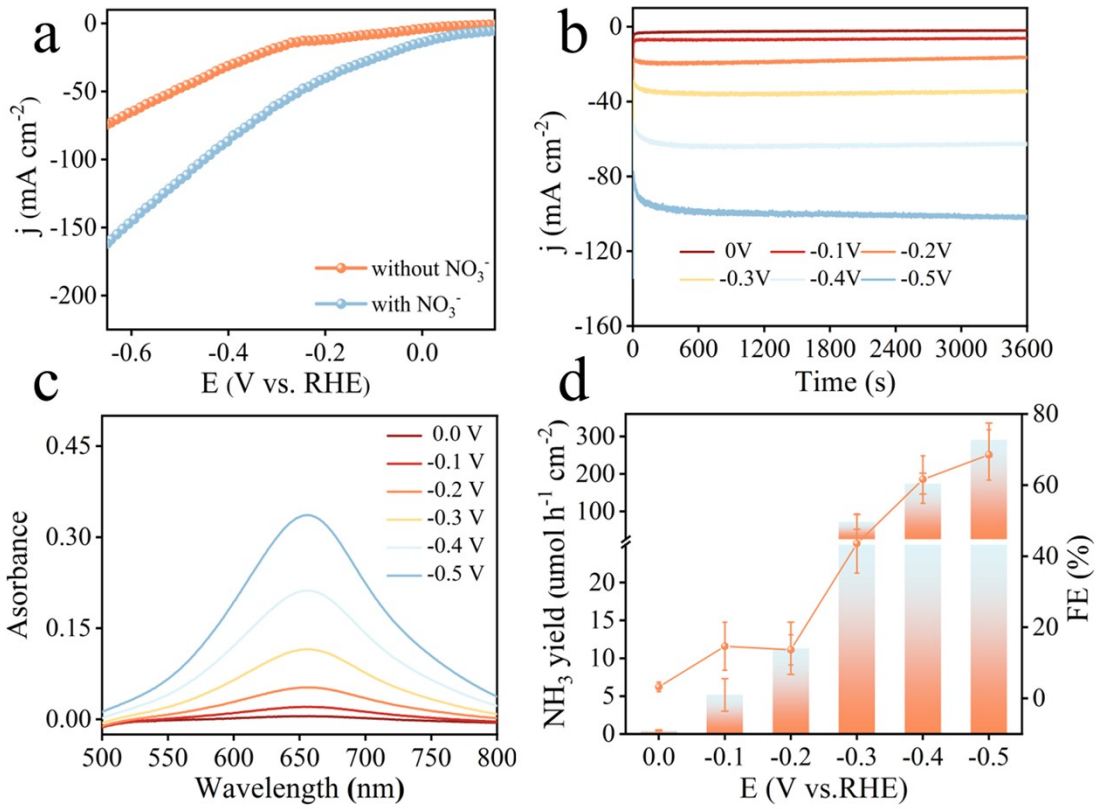

Fig. S11. (a) LSV curves of Ir@$Co(OH)_2$/TM, $Co(OH)_2$/TM and TM in neutral medium; (b) The chronoamperometry test curves of Ir@$Co(OH)_2$/TM at each given potential in neutral medium. (c) UV-vis spectra of produced NH_3; (d) NH_3 yields and FEs of Ir@$Co(OH)_2$/TM from 0 V to -0.5 V.

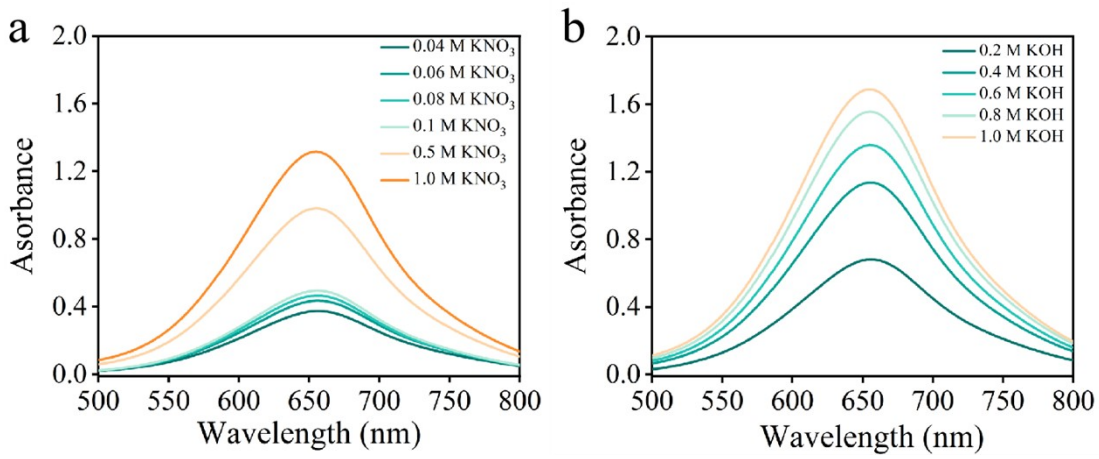

Fig. S12. UV-Vis spectra of NH_3 generated on Ir@$Co(OH)_2$/TM at different; (a) C_{NO3-} (b) C_{OH-}

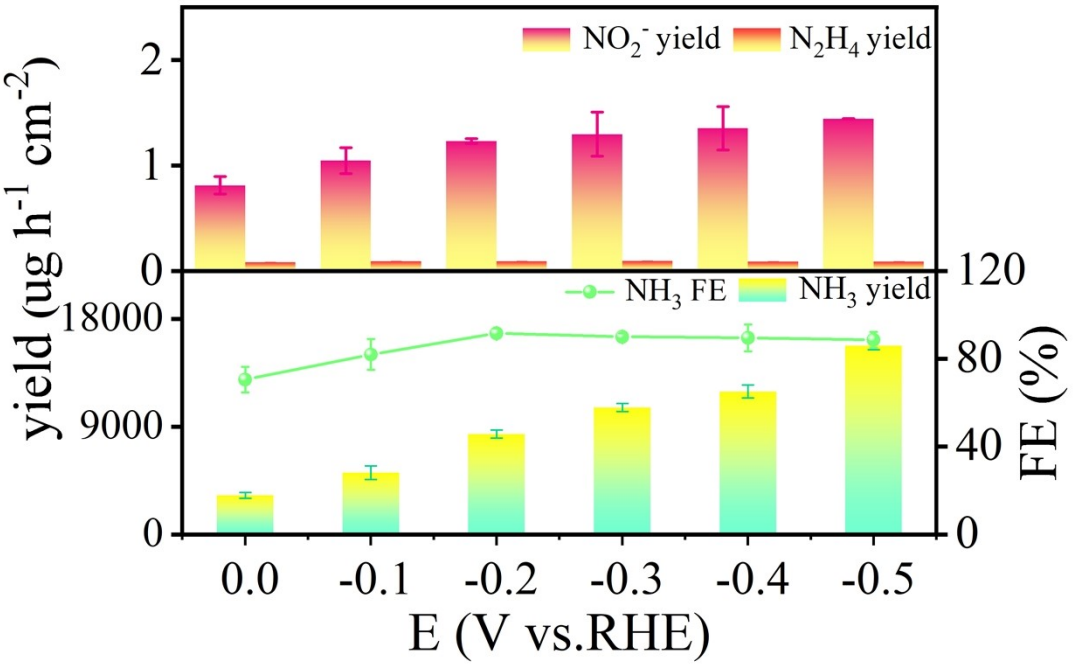

Fig. S13. By-product yield and FEs.

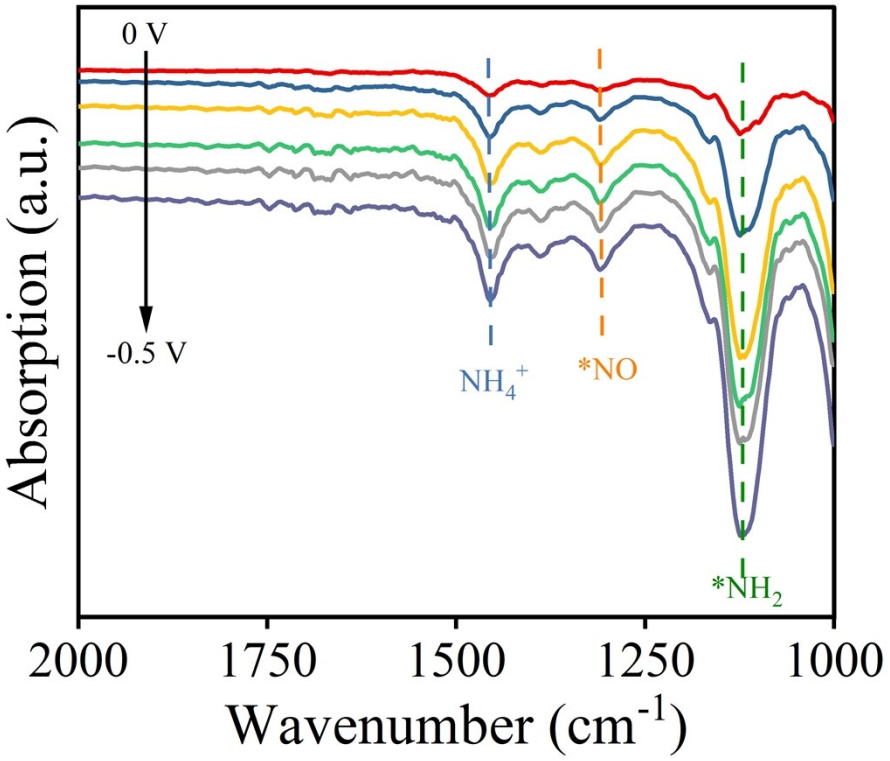

Fig. S14. Fourier transform infrared spectroscopy (FTIR) tests on Ir-$Co(OH)_2$/TM at various potentials within an alkaline NO_3^- medium

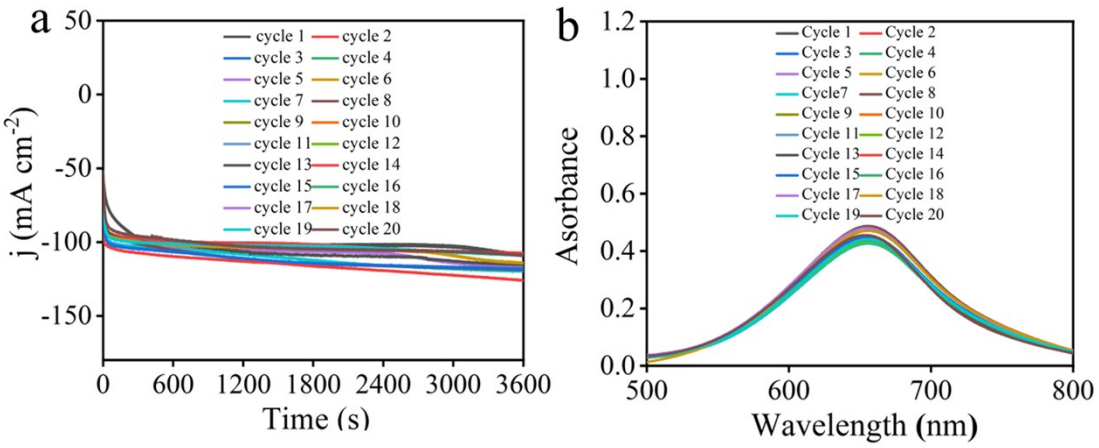

Fig. S15. (a) Chronoamperometry curves and (b) corresponding UV-Vis absorption spectra of Ir@$Co(OH)_2$/TM for generated NH_3 during cycling tests at -0.2 V.

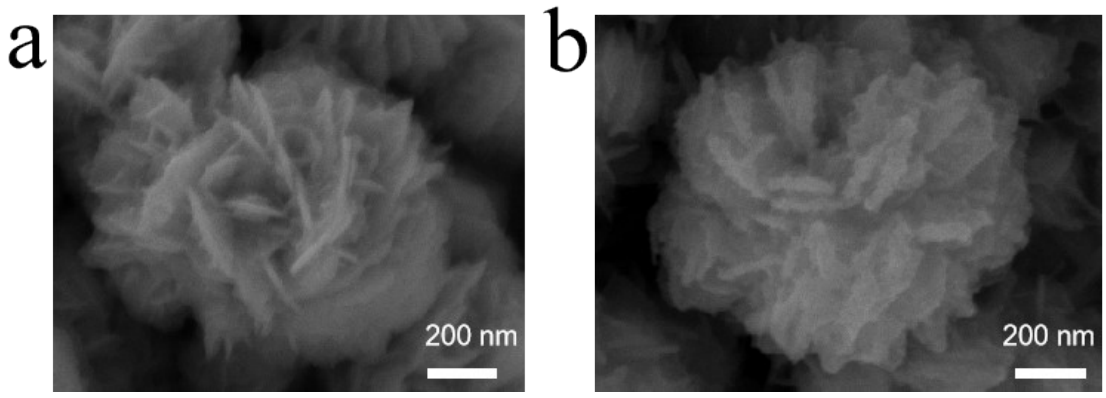

Fig. S16. SEM image of Ir@$Co(OH)_2$/TM (a) before the 24-h stability test; (b) after the 24-h stability test in 0.1 M KOH with 0.1 M KNO_3.

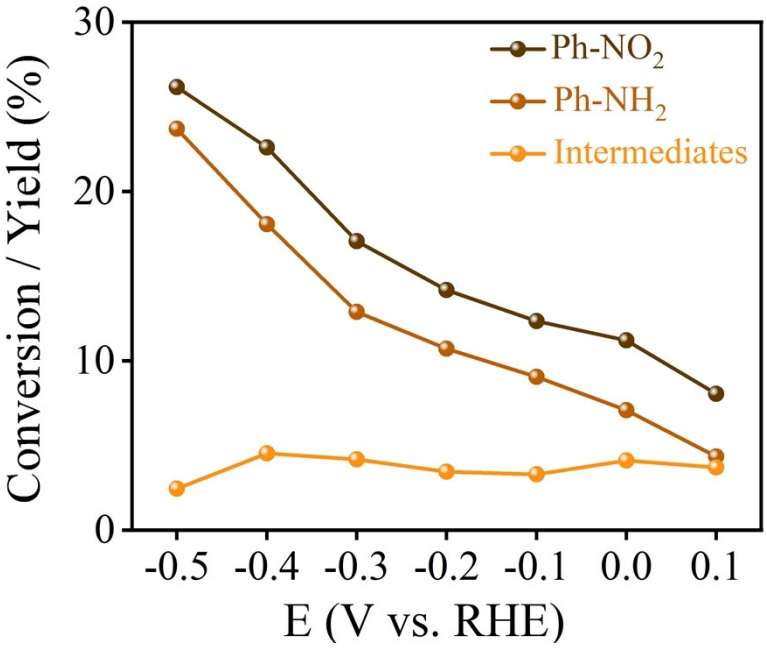

Fig. S17. Conversion and yield for Ph-NO_2 ERR from 0 V to -0.5 V

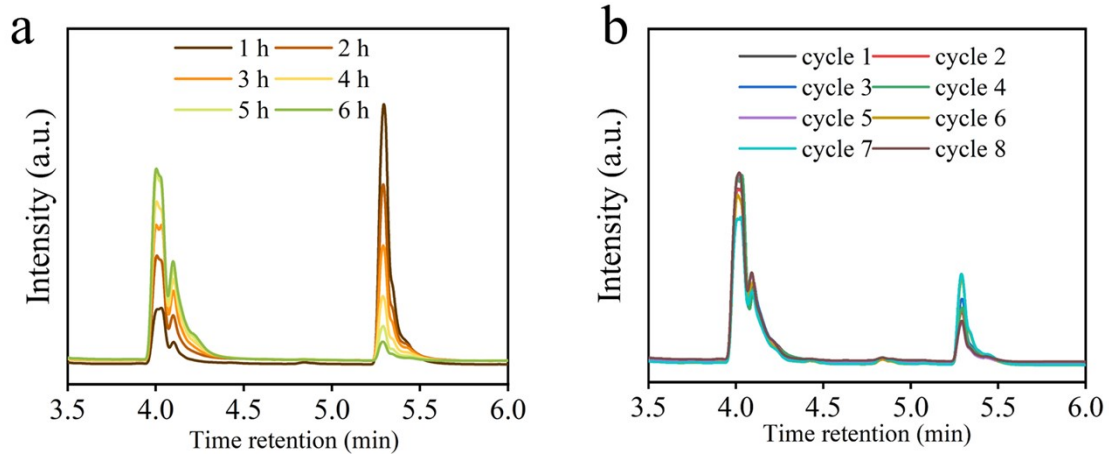

Fig. S18. (a) GC results for Ph-NO_2 ERR of Ir@$Co(OH)_2$/TM at -0.5 V (vs RHE) with various time. (b) GC results for Ph-NO_2 ERR of cycling test.

Table S1. Comparison of catalytic performance of Ir@$Co(OH)_2$/TM with other reported NO_3RR electrocatalysts.

Catalyst	Electrolyte	NH_3 yield@Potential (V vs. RHE)	FE@Potential (V vs. RHE)	Ref.
Ir@$Co(OH)_2$/ TM	0.1 M KOH (0.1 M KNO_3)	493.0 ± 19.2 umol h^{-1} cm^{-2}@-0.2	91.6 ± 2.2 %@-0.2	This work
Co_3O_4/Co	0.1 M Na_2SO_4 (1000ppm $NaNO_3$)	261 μmol h^{-1} cm^{-2}@-0.8	88.7%@-0.8	[4]
Co/CoO NSA	0.1 M Na_2SO_4 (3.23 mM $NaNO_3$)	195 μmol h^{-1} cm^{-2}@-0.65	93.8%@-0.65	[5]
Co_2B@Co_3O_4/ TM	0.1 M NaOH (0.1 M $NaNO_3$)	301.8 μmol h^{-1} cm^{-2}@-0.7	97.0%@-0.70	[6]
Co-Fe@Fe_2O_3	0.1 M Na_2SO_4 (500 ppm NO_3^-)	88 μmol h^{-1} cm^{-2}@-0.75	85.2%@-0.75	[7]
Co-NCNT	0.1 M NaOH (0.1 M NO_3^-)	350 μmol h^{-1} $mg_{cat.}^{-1}$@-0.6	92.0%@-0.6	[8]
Co@CC	0.1 M NaOH (0.1 M $NaNO_3$)	600 μmol h^{-1} cm^{-2}@-0.8	93.4%@-.8	[9]
Cu	1 M NaOH (0.1 M NO_3^-)	/	79.0%	[10]
$ZnCo_2O_4$	0.1 M KOH (0.1 M NO_3^-)	120 μmol $h^{-1}mg_{cat.}^{-1}$@-0.6	95.4%@-0.4	[11]
$Cu_{2-x}S/MoS_2$	0.5 M Na_2SO_4 (100 ppm NO3$^-$)	178 μmol h^{-1} cm^{-2}@-0.1	84.5%@-0.1	[12]
Co/MWCNTs	0.1 M KOH (0.1 M NO_3^-)	237 μmol h^{-1} cm^{-2}@-0.16	84.72%@-0.16	[13]
BCN@Ni	0.1 M KOH (0.1 M NO_3^-)	140 μmol h^{-1} cm^{-2}@-0.5	91.2%@-0.3	[14]
Cu/Cu_2O/RuO_2@ C	0.1 M NaOH (0.1 M NO_3^-)	209.4 μmol h^{-1} cm^{-2}@-0.6	82.4%@-0.6	[15]
La-Co_3O_4/CC	0.1 M NaOH (100 mM NO_3^-)	537.44 μmol h^{-1} cm^{-2}@-0.4	96.34%@-0.4	[16]
$NiCoO_2$@Cu	0.1 M KOH (0.1 M NO_3^-)	349.6 μmol h^{-1} cm^{-2}@-0.9	94.2%@-0.9	[17]
CoPc/CNT	0.1 M NaOH (0.1 M NO_3^-)	/	70%@-0.37	[18]
$Cu_{50}Ni_{50}$	0.1 M NaOH (10 mM NO_3^-)	/	84.0 ± 2.0%	[19]
VCu-Au_1Cu SAAS	0.1 M NaOH (7.14 mM NO_3^-)	32.6 μmol h^{-1} cm^{-2}@-0.2	98.7%@-0.2	[20]

Fe_2P@NiP_2	0.2 M Na_2SO_4 (0.05 M $NaNO_3$)	395 μmol h^{-1} cm^{-2}@-0.7	97.2%@-0.7	[21]
1-Cu/CC	0.1 M NaOH (0.1 M $NaNO_3$)	66 μmol h^{-1} cm^{-2}@-0.9	85.4%@-0.9	[22]
Cu/Ce_2O_3	0.1 M NaOH (0.01 M $NaNO_3$)	386 μmol h^{-1} cm^{-2}@-1.2	73.0%@-1.2	[23]

References

[1] D. Zhu, L.H. Zhang, R.E. Ruther, R.J. Hamers, Photo-illuminated diamond as a solid-state source of solvated electrons in water for nitrogen reduction, Nat. Mater. 12(9) (2013) 836-841.

[2] L. C. Green, D. A. Wagner, J. Glogowski, P. L. Skipper, J. S. Wishnok and S. R. Tannenbaum, Tannenbaum, Analysis of nitrate, nitrite, and [15N] nitrate in biological fluids, Anal. Biochem., 126 (1982) 131-138.

[3] B. Deepa, N. Balasubramanian, K.S. Nagaraja, Spectrophotometric determination of hydrazine, Asian J. Chem. 17(2) (2005) 1140-1146.

[4] F.L. Zhao, G.T. Hai, X. Li, Z.Y. Jiang, H.H. Wang, Enhanced electrocatalytic nitrate reduction to ammonia on cobalt oxide nanosheets via multiscale defect modulation, Chem. Eng. J. 461 (2023) 10.

[5] Y. Yu, C.H. Wang, Y.F. Yu, Y.T. Wang, B. Zhang, Promoting selective electroreduction of nitrates to ammonia over electron-deficient Co modulated by rectifying Schottky contacts, Sci. China-Chem. 63(10) (2020) 1469-1476.

[6] L.S. Xie, S.J. Sun, L. Hu, J. Chen, J. Li, L. Ouyang, Y.S. Luo, A.A. Alshehri, Q.Q. Kong, Q. Liu, X.P. Sun, In Situ Derived Co_2B Nanosheet Array: A High-Efficiency Electrocatalyst for Ambient Ammonia Synthesis via Nitrate Reduction, ACS Appl. Mater. Interfaces (2022) 8.

[7] S. Zhang, M. Li, J.C. Li, Q.N. Song, X. Liu, High-ammonia selective metal-organic framework-derived Co-doped Fe/Fe_2O catalysts for electrochemical nitrate reduction, Proc. Natl. Acad. Sci. U. S. A. 119(6) (2022) 11.

[8] J. Chen, Q. Zhou, L.C. Yue, D.L. Zhao, L.C. Zhang, Y.S. Luo, Q. Liu, N. Li, A.A. Alshehri, M.S. Hamdy, F. Gong, X.P. Sun, Co-NCNT nanohybrid as a highly active catalyst for the electroreduction of nitrate to ammonia, Chem. Commun. 58(23) (2022) 3787-3790.

[9] T. Xie, X.H. Li, J. Li, J. Chen, S.J. Sun, Y.S. Luo, Q. Liu, D.L. Zhao, C.G. Xu, L.S. Xie, X.P. Sun, Co Nanoparticles Decorated Corncob-Derived Biomass Carbon as an Efficient Electrocatalyst for Nitrate Reduction to Ammonia, Inorg. Chem. 61(35) (2022) 14195-14200.

[10] D. Reyter, G. Chamoulaud, D. Bélanger, L. Roué, Electrocatalytic reduction of nitrate on copper electrodes prepared by high-energy ball milling, J. Electroanal. Chem. 596(1) (2006) 13-24.

[11] P.P. Huang, T.T. Fan, X.T. Ma, J.G. Zhang, Y.P. Zhang, Z. Chen, X.D. Yi, 3D Flower-Like Zinc Cobaltite for Electrocatalytic Reduction of Nitrate to Ammonia under Ambient Conditions, ChemSusChem 15(4) (2022) 9.

[12] T.Y. Jiang, Y.H. Liu, D.X. Zhang, Q.T. Chen, L.X. Li, N.Y. Liu, C.X. Zhou, L.H. Li, B.D. Mao, Core-Shell Engineering Boosted Active Hydrogen Generation in $Cu_{2-x}S/MoS_2$ Quantum Dots for Efficient Electrocatalytic Nitrate Reduction to Ammonia, ACS Sustain. Chem. Eng. 12(15) (2024) 5979-5990.

[13] M.H. Ye, X.L. Jiang, Y.G. Zhang, Y. Liu, Y.X. Liu, L. Zhao, Enhanced Electrocatalytic Nitrate Reduction to Ammonia Using Functionalized Multi-Walled Carbon Nanotube-Supported Cobalt Catalyst, Nanomaterials 14(1) (2024) 15.

[14] X. Zhao, Z. Zhu, Y.N. He, H.B. Zhang, X.H. Zhou, W.B. Hu, M. Li, S.S. Zhang,

Y.M. Dong, X. Hu, A. Kuklin, G. Baryshnikov, H. Ågren, T. Wågberg, G.Z. Hu, Simultaneous anchoring of Ni nanoparticles and single-atom Ni on BCN matrix promotes efficient conversion of nitrate in water into high-value-added ammonia, Chem. Eng. J. 433 (2022) 12.

[15] A.M. Liu, G.X. Li, J.H. Cao, F. Zhao, X.R. Chen, Q.Q. Hua, L.G. Gao, T.L. Ma, X.F. Ren, Preparation of Ru-doped Cu-based catalysts for enhanced electrochemical ammonia synthesis from efficient electrocatalytic nitrate reduction, Catal. Sci. Technol. 13(21) (2023) 6313-6320.

[16] X. He, T. Xie, K. Dong, J. Nan, H. Sun, Y.C. Yao, X.Y. Fan, D.D. Zheng, Y.S. Luo, S.J. Sun, Q. Liu, L.M. Li, W. Chu, L.S. Xie, Q.Q. Kong, X.P. Sun, Enhancing nitrate electroreduction for ammonia production over electron-deficient Co_3O_4 with La doping regulation, Sci. China-Mater. (2024) 8.

[17] Y. Hai, X.M. Li, Y. Cao, X.Y. Wang, L.H. Meng, Y. Yang, M. Luo, Ammonia Synthesis via Electrocatalytic Nitrate Reduction Using $NiCoO_2$ Nanoarrays on a Copper Foam, ACS Appl. Mater. Interfaces 16(9) (2024) 11431-11439.

[18] N.J. Harmon, J. Li, B.T. Wang, Y.Z. Gao, H.L. Wang, Influence of Carbon Nanotube Support on Electrochemical Nitrate Reduction Catalyzed by Cobalt Phthalocyanine Molecules, ACS Catal. 14(5) (2024) 3575-3581.

[19] Y.H. Wang, A. Xu, Z.Y. Wang, L.S. Huang, J. Li, F.W. Li, J. Wicks, M.C. Luo, D.H. Nam, C.S. Tan, Y. Ding, J.W. Wu, Y.W. Lum, C.T. Dinh, D. Sinton, G.F. Zheng, E.H. Sargent, Enhanced Nitrate-to-Ammonia Activity on Copper-Nickel Alloys via Tuning of Intermediate Adsorption, J. Am. Chem. Soc. 142(12) (2020)

5702-5708.

[20] Y.Z. Zhang, X. Chen, W.L. Wang, L.F. Yin, J.C. Crittenden, Electrocatalytic nitrate reduction to ammonia on defective Au_1Cu (111) single-atom alloys, Appl. Catal. B-Environ. 310 (2022) 11.

[21] Y.N. Zheng, Y. Tan, X. Yu, H. Yao, S.J. Hu, J. Hu, Z. Chen, X.H. Guo, Optimized Intermediates Adsorption Configuration on Co-Doped Fe_2P@NiP_2 Heterojunction Interface for Enhanced Electrocatalytic Nitrate-To-Ammonia Conversion, Small (2024) 10.

[22] Y.T. Xu, M.Y. Xie, H.Q. Zhong, Y. Cao, In-Situ Clustering of Single-Atom Copper Precatalysts in a Metal-Organic Framework for Efficient Electrocatalytic Nitrate-to-Ammonia Reduction, ACS Catal. 12(14) (2022) 8698-8706.

[23] D. Li, F. Wang, J. Mao, Surface-Reconstructed Copper Foil Free-Standing Electrode with Nanoflower Cu/Ce_2O_3 by In Situ Electrodeposition Reduction for Electrocatalytic Nitrate Reduction to Ammonia, Inorg. Chem. 62(40) (2023) 16283-16287.